J. Plasma Physics (1997), *vol.* 57, *part* 3, *pp.* 515–522. Printed in the United Kingdom
© 1997 Cambridge University Press

Evolution of a preformed electron beam propagating through a conducting cylinder

HAN S. UHM

Naval Surface Warfare Center, 9500 MacArthur Boulevard, West Bethesda, Maryland 20817-5700, USA

(Received 25 August 1995 and in revised form 12 April 1996)

A theory of current and energy modulations in an electron beam propagating through a grounded drift tube is developed. The theoretical analysis is based on the assumption that each beam segment has a prescribed current profile at the drift-tube entrance. It is shown that the current modulation amplitude decreases, reaches its minimum value and increases as the beam propagates downstream. The current modulation in the linear regime is described by a sum of the forward and backward density waves. On the other hand, the energy modulation in the linear regime is described by the difference between the forward and backward density waves.

1. Introduction

Prebunched charged particle beams have various applications, including accelerator physics (Chen *et al.* 1985; Rosenzweig and Chen 1989; Rosing *et al.* 1991; Uhm 1993), relativistic klystron amplifiers (Friedman *et al.* 1988, 1990; Uhm 1993, 1994) and the high-power travelling-wave tube (TWT) (Kodis *et al.* 1990, 1991). The prebunched beam train may provide compact travelling-wave tubes, eliminating the amplification regions. A recent experiment on the micro field emission gate indicates a strong possibility of prebunched beam trains in the near future (Kodis *et al.* 1990, 1991). Unlike the klystron amplifier, which is initiated by energy modulation at the input cavity, the prebunched TWT is operated by a premodulated electron beam, where the initial current modulation is a driving factor. In this article, we develop a self-consistent nonlinear theory of a prebunched electron beam propagating through a drift tube. When the beam enters the tube, the initial electron current of the beam is modulated according to a prescribed current profile $f(\omega t_0)$, where ω is the bunching frequency of the beam and t_0 is the entering time of each beam slice. The prebunched beam particles move downstream with travelling waves of electric potential caused by non-uniform charge distribution along the propagation direction. Particles ahead of the charge bunch are accelerated and particles behind the bunch are decelerated, developing energy modulation. Eventually, the current modulation is reduced and energy modulation is increased. Further downstream, the energy modulation drives the current modulation. For example, a late beam segment with high energy catches up with an early beam segment with low energy, building a current bunch. In an ideal case, the current and energy modulations will alternate with each other as

https://doi.org/10.1017/S0022377897005370 Published online by Cambridge University Press

the beam propages downstream. However, in reality, nonlinear processes occur, driving jittering motions in particles.

2. Self-consistent evolution of premodulated current

A premodulated electron beam enters a drift tube at $z = 0$. For simplicity in the subsequent analysis, we assume that the electron beam current at $z = 0$ is premodulated according to a periodic function $f(\theta)$. Here the normalized time $\theta = \omega t_0$ represents the time t_0 at which the beam segment labelled by t_0 enters the drift tube. The function $f(\theta)$ can be an arbitrary function that represents the initial current modulation. For example, the function $f(\theta) = 1-\alpha\cos\theta$ shows a sinusoidal current modulation with modulation strength α. Because the modulation frequency ω is less than the cutoff frequency of the drift tube, the phase velocity of the self-electric and self-magnetic fields is the same as the beam velocity for a relatively tenuous beam characterized by

$$\frac{\nu}{\gamma_b} = \frac{-eI_b}{m\gamma_b\beta_b c^3} \ll 1, \tag{1}$$

where ν is Budker's parameter, I_b is the average beam current, $\gamma_b = (1-\beta_b^2)^{-1/2}$ is the relativistic mass factor of electrons, c is the speed of light in vacuum, and $-e$ and m are the charge and rest mass respectively of electrons. The vacuum permittivity is $\mu = 1$ in c.g.s. units. (The subsequent analysis is expressed in terms of c.g.s. units.) We also make use of the long-wavelength approximation, where the characteristic axial wavenumber k_z is less than the inverse of the characteristic beam radius R_b, i.e.

$$k_z R_b < 1. \tag{2}$$

The long-wavelength approximation in (2) is good for the fundamental mode number, but it may fail for describing the current modulations due to high-harmonic perturbations.

For convenience in the subsequent analysis, we define the normalized current $F(\zeta,\theta)$ by

$$F(\zeta,\theta) = \frac{I(\zeta,\theta)}{I_b}, \tag{3}$$

where I_b is the average beam current in one period of the current modulation at the injection point and the normalized distance ζ is defined by $\zeta = \omega z/\beta_b c$. The instantaneous relativistic mass factor $\gamma(\zeta,\theta)$ of the beam segment θ at ζ is approximately expressed as (Uhm 1994)

$$\gamma = \gamma_b + \frac{S}{\gamma_b^2}\int_0^{\zeta} d\zeta' \left(\frac{\partial F}{\partial}\right)_{\zeta'} \tag{4}$$

when the mass factor γ is close to the injection value of γ_b. In (4), the parameter $S = 2\nu G$ represents the beam intensity (ν in (1)) and the geometrical factor G, and $= \omega t$ is the normalized present time in which the segment θ arrives at ζ. For convenience in the subsequent analysis, we introduce the energy modulation parameter

$$K = \frac{\gamma-1}{\gamma_b-1}. \tag{5}$$

https://doi.org/10.1017/S0022377897005370 Published online by Cambridge University Press

The relation between the injection time θ and the present time is obtained by making use of the velocity definition $dz/dt = \beta c$, and the definitions of $\theta = \omega t_0$ and $= \omega t$. After some straightforward algebra, we obtain

$$-\theta = \int_0^{\zeta} \frac{\beta_b}{\beta} d\zeta' = \frac{(\gamma_b^2 - 1)^{1/2}}{\gamma_b} \int_0^{\zeta} d\zeta' \frac{\gamma}{(\gamma^2 - 1)^{1/2}}, \tag{6}$$

where $\zeta = \omega z/\beta_b c$. Substituting (4) into (6) and making use of the approximation $\gamma \approx \gamma_b$, we find

$$\left(\frac{\partial}{\partial\theta}\right)_{\zeta} = 1 - \frac{S}{\gamma_b^3(\gamma_b^2 - 1)} \int_0^{\zeta} d\zeta' \int_0^{\zeta'} d\zeta'' \left[\frac{\partial}{\partial\theta}\left(\frac{\partial F}{\partial}\right)\right]_{\zeta''}. \tag{7}$$

Note that the derivative ∂ $/\partial\theta$ in (7) is uniquely described by the history of the current modulation F before the present time in which the beam segment labelled by θ arrives at the distance z.

The beam current at the injection point is $I_b f(\theta)$ by definition, where the premodulation profile $f(\theta)$ of the beam current at the beginning is normalized by

$$\int_0^{2\pi} f(\theta)\, d\theta = 2\pi. \tag{8}$$

The beam segment t_0 passes the injection point at time $t = t_0$. When this segment arrives at z in time t, it is stretched by a factor of dt/dt_0. Thus the beam current of the segment t_0 at z is proportional to $(d\theta/d\ )f(\theta)$. In this regard, the normalized current ratio $F(\zeta, \theta)$ in (3) is expressed as

$$F(\zeta, \theta) = \frac{N(\zeta) f(\theta)}{|d\ /d\theta|}, \tag{9}$$

where the normalization constant $N(\zeta)$ is defined by

$$\frac{2\pi}{N(\zeta)} = \int_0^{2\pi} d\theta \left|\frac{d\theta}{d} f(\theta)\right|. \tag{10}$$

The normalization constant $N(\zeta)$ ensures charge conservation. Thus the current modulation is finally given by

$$\frac{N(\zeta)}{F(\zeta, \theta)} f(\theta) = \left|1 - \frac{S}{2\gamma_b^3(\gamma_b^2 - 1)} \int_0^{\zeta} dy \int_0^{y} \frac{dx}{N(x)} \frac{\partial}{\partial\theta}\left[\frac{1}{f(\theta)} \frac{\partial}{\partial\theta} F^2(x, \theta)\right]_x\right|, \tag{11}$$

which can be equivalently expressed in the single integral form

$$\frac{N(\zeta)}{F(\zeta, \theta)} f(\theta) = \left|1 - \frac{S}{2\gamma_b^3(\gamma_b^2 - 1)} \int_0^{\zeta} dx \frac{\zeta - x}{N(x)} \frac{\partial}{\partial\theta}\left[\frac{1}{f(\theta)} \frac{\partial}{\partial\theta} F^2(x, \theta)\right]_x\right|. \tag{12}$$

In obtaining (12), we have made the assumption that the energy modulation throughout the beam propagation is very small, i.e. $\gamma(\zeta, \theta) \approx \gamma_b$. That is, $|K - 1| < 0.2$, where K is defined in (5). Although this approximation looks like a severe limitation of the theory, (12) may still hold good for most practical applications, and may provide the essential physical properties that we seek. However, we remind the reader that the present analysis does not include energy loss due to radiation. This energy-loss effect will be discussed elsewhere.

https://doi.org/10.1017/S0022377897005370 Published online by Cambridge University Press

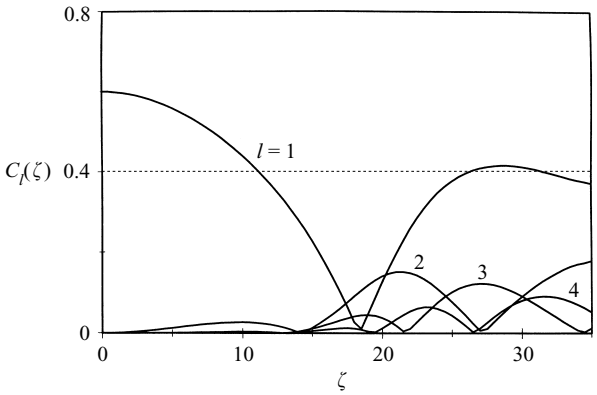


Figure 1. Plots of mode strength c_l versus propagation distance ζ obtained from (12) for an initial modulation $f(\theta) = 1 - 0.6\cos\theta$, a beam energy $\gamma_b = 1.2$, $S = 0.005$ and the first few mode numbers.

In order to investigate nonlinear evolution of the current profile, we Fourier-decompose the current modulation $F(\zeta, \theta)$ in (12) with mode strength $c_l(\zeta)$.

As an example, we consider a case where the injection beam energy $\gamma_b = 1.2$ and the parameter $S = 0.005$. The initial current modulation in Fig. 1 is assumed to be

$$f(\theta) = 1 - 0.6\cos\theta.$$

Figure 1 shows plots of the mode strength c_l versus propagation distance ζ obtained from (12). The strength of the fundamental mode ($l = 1$) indicates a decreasing cosine oscillation. At the beginning of propagation, the fundamental mode dominates because of the initial current modulation. The second and higher harmonics show up in the late stage of propagation. The mode profiles in the propagation range satisfying $0 < \zeta < 35$ are very predictable and orderly. As the beam segment propagates further downstream, nonlinear mode coupling occurs, pumping the energy into high harmonics. Eventually, particles cross over among themselves. Once the particles start to cross each other, they create many local singularities and high-frequency oscillations in the electric fields, which drive jittering motions in particles. We remind the reader that the high-harmonic modes appear as the propagation distance ζ approaches $\zeta = 35$ in Fig. 1. Numerical solution of (12) in this regime requires very fine integration steps in time and space to resolve the density and energy modulations. Otherwise, accumulation of numerical errors will obscure real physical quantities. In this regard, we stop the numerical calculation beyond the propagation distance $\zeta = 35$, which corresponds to $z = 1.5$ m for $\gamma_b = 1.2$ and 1 GHz oscillation frequency. The propagation distance of $z = 1.5$ m is more than enough for most practical applications.

Figure 2 shows plots of (a) the normalized current profile $F(\zeta, \theta)$ and (b) the energy modulation parameter $K(\zeta, \theta)$ versus the normalized time θ obtained from (5) and (12) for several different propagation distances ζ and parameters otherwise identical to those in Fig. 1. There is a strong current modulation in the early stage of propagation, which has been set by initial modulation (see the plot for $\zeta = 1$ in Fig. 2a). Comparing plots of $\zeta = 1$ in Figs 2 (a) and (b), we note that particles behind the peak current slow down, reducing their energy, and particles ahead of the peak current speed up, increasing their kinetic energy.

https://doi.org/10.1017/S0022377897005370 Published online by Cambridge University Press

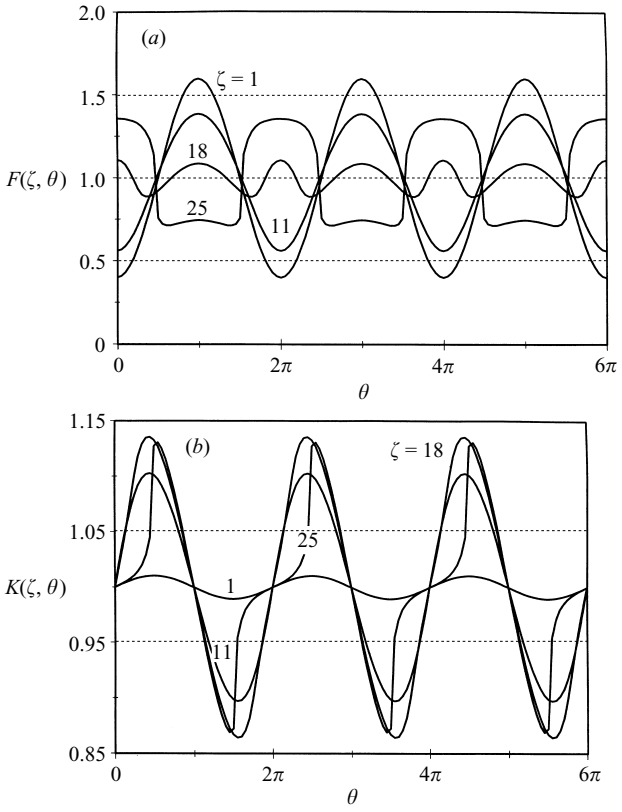


Figure 2. Plots of (*a*) the normalized current modulation $F(\zeta, \theta)$ and (*b*) the energy modulation $K(\zeta, \theta)$ versus the normalized time θ obtained from (5) and (12) for several different values of the propagation distance ζ and parameters otherwise identical to those in Fig. 1.

Obviously, the initial current modulation drives the energy modulation, which is uniform at the beginning. This process continues through the propagation distance of $\zeta = 18$ in Fig. 2(*b*). As the beam segment propagates further downstream, the current modulation reduces to a minimum and the energy modulation achieves its maximum (see plots for $\zeta = 18$ in Figs 2(*a*) and (*b*), where only the second and high harmonics of the current modulation show up). The maximum value of the energy modulation parameter K in this example is in the range of $0.85 < K < 1.15$, which translates into $1.17 < \gamma < 1.23$. Obviously, the instantaneous mass factor γ is very close to its initial value of $\gamma_b = 1.2$ throughout the beam propagation. In reality, the instantaneous mass factor γ is very close to the initial value γ_b in most experimental applications, as shown in this example. If there is enough variation in the kinetic energy as shown in the plot of $\zeta = 18$ in Fig. 2(*b*), the late-segment particles with high energy overtake the early-segment particles with low energy, increasing the current density near the time θ satisfying $(\partial\gamma/\partial\theta)_\zeta > 0$. As the beam segment propages further downstream, the current density near this time θ increases considerably, as shown in the plot for $\zeta = 25$ in Fig. 2(*a*).

https://doi.org/10.1017/S0022377897005370 Published online by Cambridge University Press

3. Linear theory

Although we have studied the current modulation in (12) numerically, it is instructive to investigate (12) analytically, in order to find simple scaling laws of premodulated beam propagation. For simplicity in the subsequent analysis, we assume a small level of modulation in the beam current, thereby defining

$$\left.\begin{aligned} f(\theta) &= 1+\delta f(\theta), \qquad 0<\theta<2\pi, \\ F(\zeta,\theta) &= 1+\delta F(\zeta,\theta), \end{aligned}\right\} \tag{13}$$

where the amplitudes of δf and δF are much less than unity. The function $\delta f(\theta)$ in (13) is defined in the range $0<\theta<2\pi$. The initial current profile $f(\theta)$ in (13) must satisfy the normalization condition in (8), which means that the average value of the function $\delta f(\theta)$ over one period must be zero. At the beginning, we describe the current modulation in the primary range of $0<\theta<2\pi$, and then we extend the theory for the whole range. Substituting (13) into (11) and linearizing, we find

$$\delta F(\zeta,\theta) = \delta f(\theta) + \eta^2 \int_0^\zeta dy \int_0^y dx \left[\frac{\partial^2}{\partial\theta^2}\delta F(x,\theta)\right]_x, \tag{14}$$

where the frequency η of the amplitude oscillation is defined by

$$\eta^2 = \frac{S}{\gamma_b^3(\gamma_b^2-1)}, \tag{15}$$

and the normalization constant $N(\zeta)$ in (10) has been approximated by $N(\zeta)=1$ for small oscillations.

Differentiating both sides of (14) with respect to ζ, we obtain

$$\frac{\partial^2}{\partial\zeta^2}\delta F(\zeta,\theta) = \eta^2\frac{\partial^2}{\partial\theta^2}\delta F(\zeta,\theta), \tag{16}$$

which is a typical equation for wave propagation. The physically acceptable solution of (16) is

$$\delta F(\zeta,\theta) = AH(\theta+\eta\zeta) + BH(\theta-\eta\zeta), \tag{17}$$

where the function $H(x)$ and the coefficients A and B must be determined from the boundary conditions.

In general, we assume that the beam current has its premodulated form $\delta f(\theta)$ at $\zeta=0$ and the current modulation waves associated with this premodulated form propagate from $\zeta=0$ to $\zeta=\pm\infty$. The function $\delta F(\zeta,\theta)$ satisfying (14) is an even function of the variable ζ. Because of the initial condition that $\partial\delta F/\partial\zeta=0$ in (14) at $\zeta=0$, we note that $A=B$ in (17). From the boundary condition that $\delta F(\zeta,\theta)=\delta f(\theta)$ at $\zeta=0$, we also note that $A=\frac{1}{2}$ and $H(\theta)=\delta f(\theta)$. Therefore the linear solution of (17) is given by

$$\delta F(\zeta,\theta) = \tfrac{1}{2}[\delta f(\theta+\eta\zeta)+\delta f(\theta-\eta\zeta)]. \tag{18}$$

The premodulated beam at $\zeta=0$ is periodic with periodicity 2π. Therefore the current modulation $\delta F(\zeta,\theta)$ at $\zeta=0$ is expressed as

$$\delta F(0,\theta) = \sum_{n=-\infty}^{\infty} \delta f(\theta-2n\pi), \tag{19}$$

https://doi.org/10.1017/S0022377897005370 Published online by Cambridge University Press

where the function $\delta f(x)$ is defined in the range $0 < x < 2\pi$. Therefore the modulation δF in (18) for the whole range must be expressed as

$$\delta F(\zeta, \theta) = \frac{1}{2} \sum_{n=-\infty}^{\infty} [\delta f(\theta + \eta\zeta - 2n\pi) + \delta f(\theta - \eta\zeta - 2n\pi)], \tag{20}$$

which also exhibits a periodicity of 2π.

Substituting (4) into (5), the energy modulation parameter is expressed as

$$K(\zeta, \theta) = 1 + \gamma_b(\gamma_b + 1)\,\eta^2 \int_0^{\zeta} d\zeta' \left[\frac{\partial}{\partial\theta}\delta F(\zeta', \theta)\right]_{\zeta'}. \tag{21}$$

Substituting (20) into (21) and carrying out some straightforward algebra, we obtain the parameter

$$K(\zeta, \theta) = 1 + \gamma_b(\gamma_b + 1)\,\eta\,\delta E(\zeta, \theta), \tag{22}$$

where the normalized energy modulation $\delta E(\zeta, \theta)$ is defined by

$$\delta E(\zeta, \theta) = \frac{1}{2} \sum_{n=-\infty}^{\infty} [\delta f(\theta + \eta\zeta - 2n\pi) - \delta f(\theta - \eta\zeta - 2n\pi)] \tag{23}$$

in the linear regime.

The current modulation $F(\zeta, \theta)$ in (20) is the sum of the forward and backward density waves in the linear regime. On the other hand, the energy modulation in the linear regime is the difference between the forward and backward density waves, as shown in (23). The amplitude oscillation frequency η is related to the amplitude wavelength λ by

$$\lambda = \frac{2\pi}{\eta} = 2\pi \left[\frac{\gamma_b^3(\gamma_b^2 - 1)}{S}\right]^{1/2}, \tag{24}$$

where S is proportional to the beam intensity and is related to a geometrical factor. Several points are noteworthy from (20), (23) and (24). First, the maximum current modulation occurs at the propagation distance ζ satisfying $\eta\zeta = j\pi$, where j is an integer. The forward and backward density waves at $\eta\zeta = j\pi$ have the same intensity and sign. Therefore the energy modulation at $\eta\zeta = j\pi$ is zero. Secondly, the maximum energy modulation occurs at the propagation distance ζ satisfying $\eta\zeta = (j + \frac{1}{2})\,\pi$, where the forward and backward density waves almost cancel each other and the current modulation is least. The current and energy modulations in the linear regime alternate with each other during propagation. Thirdly, the amplitude wavelength in (24) increases with beam energy and decreases with beam intensity. As an example, we consider the amplitude wavelength $\lambda = 76$ from (24) for $\gamma_b = 1.2$ and $S = 0.005$. One-quarter of the wavelength $\frac{1}{4}\lambda = 19$ agrees well with the numerical calculation $\frac{1}{4}\lambda = 17.5$ from (12) or Fig. 1 for a highly modulated initial current.

Acknowledgment

This research was supported by the Independent Research Fund at the Naval Surface Warfare Center.

References

Chen, P., Dawson, J. M., Huff, R. W. and Katsouleas, T. 1985 *Phys. Rev. Lett.* **54**, 693.

https://doi.org/10.1017/S0022377897005370 Published online by Cambridge University Press

Friedman, M., Krall, J., Lau, Y. Y. and Serlin, V. 1988 *J. Appl. Phys.* **64**, 3353.

Friedman, M., Krall, J., Lau, Y. Y. and Serlin, V. 1990 *IEEE Trans. Plasma Sci.* **18**, 553.

Kodis, M. A., Vanderplaats, N. R. and Zaidman, E. G. 1990 Technical Digest of the International Electron Devices Meeting 1990, *San Francisco, CA*, vol. I, p. 893. Institute of Electrical and Electronic Engineers, New York.

Kodis, M. A., Freund, H. P., Vanderplaats, N. R. and Zaidman, E. G. 1991 Technical Digest of the International Electron Devices Meeting 1991, *Washington, DC*, vol. I, p. 589. Institute of Electrical and Electronic Engineers, New York.

Rosenzweig, J. B. and Chen, P. 1989 *Phys. Rev.* **D39**, 2039.

Rosing, M., Chojnaki, E., Gai, W., Ho, C., Konecny, R., Mtingwa, S., Norem, J., Schoessow, P. and Simpson, J. 1991 Proceedings of the 1991 IEEE Particle Accelerator Conference, *San Francisco, CA*, vol. I, p. 555. Institute of Electrical and Electronic Engineers, New York.

Uhm, H. S. 1993 *Phys. Fluids* **B5**, 972.

Uhm, H. S. 1994 *Phys. Plasmas* **1**, 2038.

https://doi.org/10.1017/S0022377897005370 Published online by Cambridge University Press